JOURNAL OF GUIDANCE, CONTROL, AND DYNAMICS
Vol. 15, No. 5, September–October 1992

Stochastic Prediction Techniques for Wind Shear Hazard Assessment

D. Alexander Stratton* and Robert F. Stengel†
Princeton University, Princeton, New Jersey 08540

The threat of low-altitude wind shear has prompted development of aircraft-based sensors that measure winds directly on an aircraft's intended flight path. Measurements from these devices are subject to turbulence inputs and measurement error, as well as to the underlying wind profile. In this paper stochastic estimators are developed to process onboard Doppler sensor measurements, producing optimal estimates of the winds. A stochastic prediction technique determines the level of aircraft energy performance from the wind estimates. Aircraft performance degradation algorithms presented are based on optimal estimation techniques. The prediction algorithm must balance wind shear detection performance and turbulence rejection capability, as illustrated in simulations of microburst wind shear and severe turbulence environments.

Introduction

STRONG variable winds in the airport vicinity can cause unacceptable deviation of aircraft from their intended flight path. Known as low-altitude wind shear, this threat has caused at least 24 aviation accidents in the last 25 years.[1] Efforts to promote the avoidance of severe wind shear have focused on improving flight crew training programs,[2] understanding the meteorology of wind shear,[3-5] and developing technology to detect wind shear in the terminal area. Ground-based sensor systems to measure airport-vicinity winds are being developed and installed at major airports,[6,7] along with techniques to automatically identify a wind shear and predict its formation.[8-10] Sensors to detect wind-shear-induced flight-path deviations are being installed on aircraft,[11,12] and forward-looking sensors to detect wind shear in front of the aircraft also are under development.[13-15] Interpretation of this information in the cockpit is a topic of current research.

As the amount of available information grows, accurate interpretation of the information by flight crews becomes more challenging, particularly during periods of high workload. Artificial intelligence technology provides a basis for a cockpit aid to assist flight crews in avoiding low-altitude wind shear. An expert system, the Wind Shear Safety Advisor,[16] depicted schematically in Fig. 1, will operate in real time, accepting evidence from onboard and ground-based sources, perhaps facilitated by a direct data link (represented by a dotted line in Fig. 1). The goal of this system is to increase flight crew situation awareness and decision reliability by summarizing information from a variety of information sources.

In the absence of direct measurements of the winds, a decision to avoid wind shear must be based on discrete alerts from wind shear detection systems and meteorological evidence. Various levels of reliability associated with this indirect evidence complicate the risk assessment process. A probabilistic model of this process has been developed that incorporates statistics from meteorological studies and reliability statistics for wind-shear-alerting systems.[17] The model can manage the uncertainty associated with indirect evidence, providing meaningful estimates of risk.

If onboard measurements of the winds were available, a hazardous level of wind shear could be identified by determining whether the level of some hazard metric, based on the wind measurements, exceeds a threshold. Hazard metrics considered previously include maximum horizontal winds[3] and F-factor,[14] which relates wind shear to aircraft performance. Computation of the hazard level is complicated by uncertainty surrounding the wind measurements, including turbulence and measurement errors. In this paper Kalman filters are developed to produce optimal wind estimates from onboard wind sensors, based on a stochastic wind model. These algorithms are demonstrated in a simulated microburst wind shear environment.

From the wind estimates, predictions of the aircraft's performance degradation can be made using stochastic prediction techniques.[18,19] In addition to the predictions themselves, these techniques produce measures of the possible error in the predictions due to turbulence and limitations of the measurement devices. In this paper a Kalman-filter-based prediction technique to predict F-factor and aircraft performance degradation is demonstrated in simulated microburst wind shear encounter. The response characteristics of the prediction technique must provide significant response to severe wind shear and limited response to turbulence. In this paper stochastic prediction techniques with different design parameters are demonstrated in a simulated microburst wind shear and severe turbulence environments.

Probabilistic Reasoning in Artificial Intelligence

The power of an intelligent system rests in its ability to produce meaningful conclusions by reasoning, i.e., by applying knowledge stored in the system to available evidence. In probabilistic models of reasoning, knowledge is stored in the form of probabilities, and Bayes's rule[20] and the axioms of probability[21] are used to condition these probabilities on evidence. When several pieces of evidence are supplied, the application of Bayes's rule is complicated by dependencies between pieces of evidence. A structure to these dependencies must be provided for efficient reasoning. In Bayesian network representation[22] a graphical representation provides this structure, such as the one for wind shear avoidance graphed in Fig. 2. Nodes in the diagram represent discrete random variables, and the links between them represent sets of conditional probabilities used during reasoning. The network representation enables efficient probabilistic reasoning because all of the dependencies between variables are specified by the links.

The network of Fig. 2 was developed using guidelines for wind shear avoidance presented in the FAA's Windshear Training Aid document,[2] which was written by a team from

Received Feb. 12, 1991; revision received Sept. 12, 1991; accepted for publication Oct. 6, 1991.

*Research Assistant, Department of Mechanical and Aerospace Engineering. Member AIAA.

†Professor, Department of Mechanical and Aerospace Engineering. Associate Fellow AIAA.

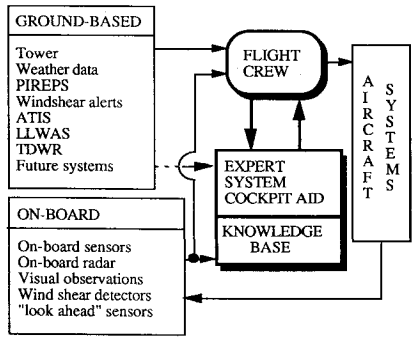

Fig. 1 Wind shear safety advisor schematic diagram.

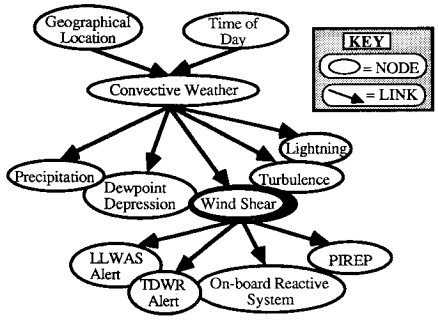

Fig. 2 Graphical representation of a Bayesian network for wind shear avoidance.

the airframe industry with the support of airlines, the government, and academia. The network model incorporates statistical results from the NIMROD,[3] JAWS,[3,4] and FLOWS[5] studies and for the enhanced Low-Level Windshear Alert System (LLWAS) evaluation.[7] Demonstrations of the network[17] show that it can approximate the subjective judgments required to establish the possible presence of wind shear.

A probabilistic model establishes a scientific basis for the Windshear Training Aid avoidance guidelines. Since the completion of the Windshear Training Aid, a variety of new ground-based and airborne wind shear detection systems are being devleoped, such as the Terminal Doppler Weather Radar (TDWR) system. The probabilistic model can be expanded to include statistics from new detection systems established during their evaluation. New knowledge gained from meteorological studies, such as geographical variation of wind shear frequency, can also be included.

Kalman Filter Development for Doppler Wind Measurements

Airborne sensor technology with the capability to detect wind shear in front of the aircraft is currently under development, including Doppler radar,[13] Doppler lidar,[14] and infrared[15] technology. Doppler devices measure a shift in frequency of radar or light waves emitted along a radial line, measuring the component of wind velocity parallel to that line. Operational devices could provide measurements of head winds or tail winds at a series of locations along the aircraft's intended approach or takeoff path. For example, airborne Doppler radars could provide measurements spaced at ~500-ft intervals over a range of 3-5 miles, spanning 50-100 s of flight at approach speed.[13] This sequence of measurements contains the effect of turbulence and is corrupted by measurement noise as well. A bank of Kalman filters can improve the accuracy of hazard estimates based on successive measurement sequences, minimizing measurement noise and accounting for correlation in the wind field using a stochastic model.

As the aircraft travels down the flight path, measurements in successive sequences are offset by a distance d (Fig. 3), which is assumed to be small relative to the distance between adjacent range gates L. At a given time, a sequence of measurements is obtained. Each member of this sequence represents the average value of the radial wind component in an interval of length L at that time.

A first-order Markov model for the turbulent winds can be based on the Dryden power spectrum for horizontal turbulence, given by Ref. 23 as

$$\Phi_u(\omega) = \left(\frac{2L_u\sigma_u^2}{\pi}\right)\frac{1}{\left[1+(L_u\omega)^2\right]} \tag{1}$$

Parameters of this model include the turbulence scale length L_u and the root-mean-square turbulence amplitude σ_u. The corresponding discrete Markov sequence is

$$w_{t_k} = \exp(-d_u)w_{t_{k-1}} + \sqrt{1-\exp(-2d_u)}\,\eta_{k-1} \tag{2}$$

where d_u is the ratio of d to L_u. The η is a normally-distributed white noise sequence with mean and variance:

$$E\{\eta_k\} = 0 \tag{3}$$

$$E\{\eta_k^2\} = \sigma_u^2/\pi \tag{4}$$

This model uses the discrete white noise sequence η to approximate the integrated effect of continuous white noise. Figure 4 presents the autocovariance function associated with Eq. (1), along with the autocovariance function of the sequence of Eq. (2), indicating the agreement of the turbulence models.

With the assumption that measurement noise is superimposed on the radial wind components, the measurement at range gate j during measurement sequence k, z_{jk} can be related

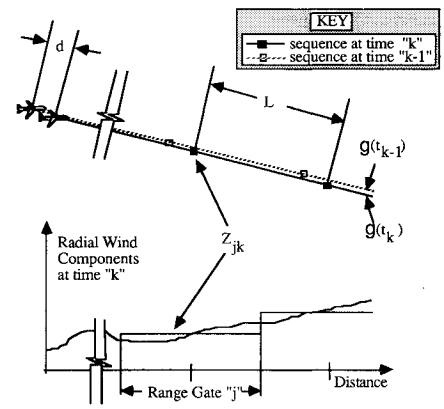

Fig. 3 Forward-look sensor measurement process.

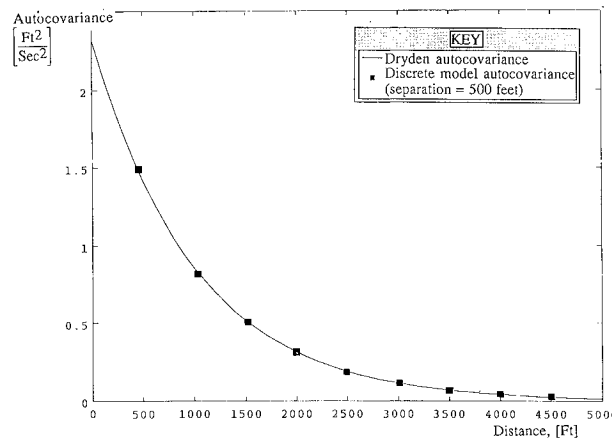

Fig. 4 Comparison of Dryden turbulence spectrum autocovariance function and autocovariance function of discrete turbulence model.

to the corresponding scalar radial wind component by the relationship

$$z_{jk} = w_{r_{jk}} + n_{jk} + V_{I_k} \tag{5}$$

This can be rewritten as

$$\tilde{z}_{jk} = w_{r_{jk}} + \tilde{n}_{jk} \tag{6}$$

where V_I is the aircraft's inertial speed at the time of measurement sequence k, and $\tilde{z}_{jk}$ has this bias subtracted out. Error in the inertial speed estimate, n_{V_I}, which is made from onboard measurements, is added to n_{jk} to produce $\tilde{n}_{jk}$:

$$\tilde{n}_{jk} = n_{jk} + n_{V_I} \tag{7}$$

The measurement error $\tilde{n}$ is assumed to be a zero-mean, normally distributed white noise sequence, with a known constant standard deviation σ_n.

With the aforementioned assumptions, an estimator dedicated to each range gate can be constructed in the form of a Kalman filter. From the measurement $\tilde{z}_{jk}$, each Kalman filter constructs an estimate $\hat{w}_{r_{jk}}(+)$ and a variance $p_{jk}(+)$, which is a measure of the uncertainty in $\hat{w}_{r_{jk}}(+)$, in three steps. First, the state estimate and variance form the previous measurement sequence, $\hat{w}_{r_{jk-1}}(+)$ and $p_{jk-1}(+)$, are extrapolated according to

$$\hat{w}_{r_{jk}}(-) = \exp(-d_u)\hat{w}_{r_{jk-1}}(+) \tag{8}$$

$$p_{jk}(-) = \exp(-2d_u)p_{jk-1}(+) + \left[1-\exp(-2d_u)\right]\sigma_u^2/\pi \tag{9}$$

Equation (8) is obtained by taking the expected value of Eq. (2). Note that Eq. (9) is an approximation to the integrated effects of continuous white noise. Next, the extrapolated variance $p_{jk}(-)$ is used to compute a gain K_{jk}:

$$K_{jk} = \frac{p_{jk}(-)}{p_{jk}(-)+\sigma_n^2} \tag{10}$$

Finally, the post-update wind estimate and variance are computed:

$$\hat{w}_{r_{jk}}(+) = \hat{w}_{r_{jk}}(-) + K_{jk}\left[\tilde{z}_{jk} - \hat{w}_{r_{jk}}(-)\right] \tag{11}$$

$$p_{jk}(+) = \left[p_{jk}(-)+\sigma_n^2\right] / \left[p_{jk}(-)\sigma_n^2\right] \tag{12}$$

The Kalman filters compute a weighted average of the wind measurements obtained at each range gate, compensating for the movement of the sensor platform by making an assumption of frozen Dryden turbulence in the interval between the measurements. Wind shear estimates are updated at each measurement step, compensating for turbulence and weighing current and prior information according to its relative uncertainty. Because each range gate's state estimator is decoupled from the others, the computation could be performed on a set of identical processors running in parallel. This decoupling is achieved as a consequence of the Markov property of the wind model: the probability distribution at a given wind state $w_{r_{jk}}$ is conditionally independent of $w_{r_{j-1k}}$ given the closer state $w_{r_{jk-1}}$. This assumption could be relaxed, coupling adjacent states or larger groups of states together with a corresponding increase in computational complexity.

Prior state estimates and variances are required to initialize each filter. This may be accomplished by applying a separate initialization Kalman filter to the first sequence of wind measurements. This filter is initialized with an onboard wind estimate and variance at the aircraft's location, perhaps from a Kalman filter processing onboard sensor measurements. An initial sequence of wind measurements from the forward-looking sensors is then processed to initialize the state and variance of each Kalman filter. The initialization Kalman filter takes the same form as Eqs. (8–12), except that the distance between range gates L is used as the distance between measurements d.

Hazard Metrics and Stochastic Prediction

The detection of the presence of a wind shear can be based on the output of the stochastic estimators. A reasonable approach to detecting wind shear is to predict whether the level of some hazard metric based on the wind estimates will exceed a threshold. The F-factor hazard metric relates wind shear to aircraft air-referenced specific energy rate, which is defined by

$$\frac{\mathrm{d}E_s}{\mathrm{d}t}(t) = \left(\frac{V_a}{g}\right)\frac{\mathrm{d}V_a}{\mathrm{d}t} + \frac{\mathrm{d}h}{\mathrm{d}t} \tag{13}$$

where V_a is the airspeed, h is aircraft altitude, and g is the gravitational constant. Using longitudinal aircraft equations of motion and assuming small flight-path angles, it can be shown[14] that

$$\frac{\mathrm{d}E_s}{\mathrm{d}t}(t) = \frac{(T-D)V_a}{W} - \mathcal{F}(t)V_a \tag{14}$$

where T is thrust, D is drag, and W is aircraft weight. $\mathcal{F}(t)$ is the F-factor, defined as

$$\mathcal{F}(t) = \left(\frac{1}{g}\right)\frac{\mathrm{d}w_x}{\mathrm{d}t}(t) - \frac{w_h(t)}{V_a} \tag{15}$$

where $w_x(t)$ is the wind component in the inertial horizontal direction, and $w_h(t)$ is the vertical wind component. For small flight-path angles, the radial wind components are approximately the same as the longitudinal horizontal wind components. Wind shear effects enter Eq. (14) in three ways: 1) by changing the airspeed, 2) by altering the drag, and 3) directly through $\mathcal{F}(t)$. For conditions typical of jet transport flight through severe wind shear, only the direct impact of $\mathcal{F}(t)$ is significant. Prediction of aircraft specific energy along the intended trajectory appears to involve the prediction of airspeed, but using a constant nominal value of airspeed in Eq. (15) introduces a small, conservative error.

The first component of $\mathcal{F}$ in Eq. (15) is proportional to the rate of change of the horizontal wind component. If the wind field is assumed stationary, prediction of $\mathcal{F}$ along the intended trajectory could be made by differencing adjacent wind estimates:

$$\hat{\mathcal{F}}_j = 1/L\left(\hat{w}_{r_{jk}} - \hat{w}_{r_{j-1k}}\right) \tag{16}$$

This would amplify high-frequency noise, resulting in excessive prediction error. Alternatively, predicted energy deviation and $\mathcal{F}$ can be computed by a Kalman filter algorithm using the wind estimates as inputs. $\mathcal{F}$ is obtained through a weighted sum of the radial wind estimates, with the weights selected by definition and minimization of a suitable cost function.

An important limitation of Doppler wind measurement devices is their inability to measure winds perpendicular to the direction of the Doppler pulse. As a consequence, the second component of $\mathcal{F}$ in Eq. (15), due to vertical winds, is not measured by the device. In downburst wind shears, head-tail wind shear is produced by vertically descending winds that flow outward as they near the ground. These downdraft winds pose a hazard to the aircraft that the Doppler sensors cannot directly measure. Current research is attempting to model the vertical wind as a function of the horizontal wind for hazard estimation.[23] In the simple downburst model of Ref. 23, the correlation between horizontal and vertical winds depends on the size of the downdraft, the altitude, and the distance from the downburst core. In a well-measured and well-studied microburst, four major downdraft regions were found.[24] As the relationship between horizontal and vertical winds remains to

be established, the present study is based on radial wind alone. If a consistent correlation between vertical wind and radial-wind measurement is found, vertical wind could be added to the stochastic model.

To predict the wind-shear-induced energy deviation E_{sw}, Eq. (14) can be integrated across a typical range gate j, resulting in the recursive form

$$E_{sw_j} = E_{sw_{j-1}} - \left(\frac{V_a L}{V_i}\right)\mathcal{F}_{j-1_{av}} \tag{17}$$

where V_i is average inertial speed of the aircraft. $\mathcal{F}_{av}$ is modeled as a stationary process driven by a discrete random sequence:

$$\mathcal{F}_{j_{av}} = \mathcal{F}_{j-1_{av}} + \eta_{j-1} \tag{18}$$

where η is a normally distributed white noise sequence with zero mean and standard deviation σ_η. This standard deviation is a design parameter that alters the response characteristics of the prediction filter, as demonstrated by simulation. Equations (17) and (18) may be written in vector-matrix form:

$$\boldsymbol{x}_j = \begin{bmatrix} 1 & -\left(\frac{V_a L}{V_i}\right) \\ 0 & 1 \end{bmatrix} \boldsymbol{x}_{j-1} + \begin{bmatrix} 0 \\ 1 \end{bmatrix} \eta_{j-1} \tag{19}$$

where

$$\boldsymbol{x}_j = \begin{bmatrix} E_{sw_j} & \mathcal{F}_{j_{av}} \end{bmatrix}^T \tag{20}$$

The relationship between prediction and estimation is obtained by substitution of Eq. (15) into Eq. (14) and integration from the aircraft (denoted with subscript 0) to a typical range gate j. This results in the equation

$$w_{x_j} - w_{x_0} = -\left(\frac{g}{V_a}\right)\left(E_{sw_j} - E_{sw_0}\right) + \left(\frac{L}{V_i}\right) w_{h_{av}} \tag{21}$$

If the prediction is initialized with the condition

$$E_{sw_0} = -(V_a/g)\, w_{x_0} \tag{22}$$

then Eq. (21) may be rewritten as

$$w_{x_j} = \begin{bmatrix} -\left(\frac{g}{V_a}\right) & 0 \end{bmatrix} \boldsymbol{x}_j + \left(\frac{gL}{V_a V_i}\right) w_{h_{av}} \tag{23}$$

In this paper vertical wind is modeled as a normally distributed white random sequence, uncorrelated with the radial winds, with mean and variance

$$E\{w_{h_j}\} = 0 \tag{24}$$

Table 1 Simulation parameters

Aircraft initial conditions	
Airspeed, V_a	160 Kt
Altitude, h	2000 ft
Inertial flight-path angle, γ_i	−3 deg
Distance to microburst core	20,100 ft
Doppler sensor	
Range gate separation, L	500 ft
Distance between sequences, d	27 ft
Noise standard deviation, σ_n	1 ft/s
Distance to aircraft	20,000 ft
Turbulence	
rms turbulence intensity, σ_u	2.7 ft/s
Turbulence scale length, L_u	1000 ft
Microburst	
Downdraft radius	2070 ft
Maximum horizontal winds	58.4 ft/s
Height of boundary layer	131 ft

and

$$E\{w_{h_j}^2\} = \sigma_{w_h}^2 \tag{25}$$

With the previously given model, prediction of the hazard level can be made from the output of the estimation Kalman filters after each measurement sequence. The wind estimates are processed using a recursive procedure based on the Kalman filter.[18,19] The prediction is initialized with onboard estimates of w_{x_0} and $\mathcal{F}_0$. Predictions of E_{sw} and $\mathcal{F}_{av}$, denoted $\hat{E}_{sw}$ and $\hat{\mathcal{F}}$, are made for each range gate using the recursive equations

$$\hat{E}_{sw_j} = \hat{E}_{sw_{j-1}} - \frac{V_i}{gL}\hat{\mathcal{F}}_{j-1} + K_{E_j}\left[\hat{w}_{r_{jk}} - \frac{g}{V_i}\hat{E}_{sw_{j-1}} - \frac{V_i}{gL}\hat{\mathcal{F}}_{j-1}\right] \tag{26}$$

$$\hat{\mathcal{F}}_j = \hat{\mathcal{F}}_{j-1} + K_{\mathcal{F}_j}\left[\hat{w}_{r_{jk}} - \frac{g}{V_i}\hat{E}_{sw_{j-1}} - \frac{V_i}{gL}\hat{\mathcal{F}}_{j-1}\right] \tag{27}$$

These equations involve two gains, K_{E_j} and $K_{\mathcal{F}_j}$, that are computed at each step based on the covariance propagation and filter gain computations of the Kalman filter.[18,19] The design parameter σ_η influences the size of these gains, influencing the response characteristics of the prediction filters.

Simulation of Stochastic Prediction Techniques

The stochastic estimation and prediction algorithms are demonstrated using a batch simulation of aircraft encounters with downburst wind shear and with severe turbulence. For each simulation, two different predictions are made, based on different choices of the design parameter σ_η. The wind shear is modeled by the Oseguera-Bowles stagnation-point-flow downburst model,[25] and severe turbulence is modeled using the Dryden spectrum as presented in Ref. 26. A twin-jet transport aircraft is represented by a point-mass longitudinal model,[27] trimmed along an approach path at a constant airspeed of 160 Kts. Normally distributed white noise is superimposed on measurements to simulate Doppler sensor error. Table 1 lists the parameters of the simulation.

The wind shear simulation is initiated with the microburst just out of the sensor's detection range. Figure 5 depicts the

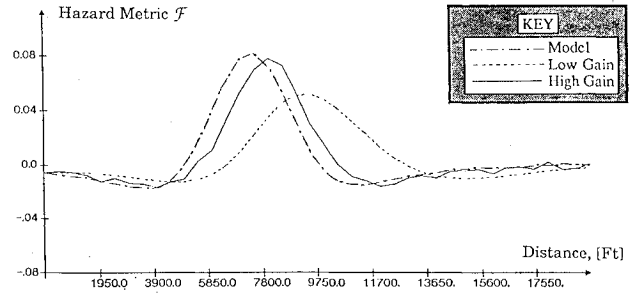

Fig. 5 Comparison of microburst model headwind-tailwind component of F-factor with predicted F-factor.

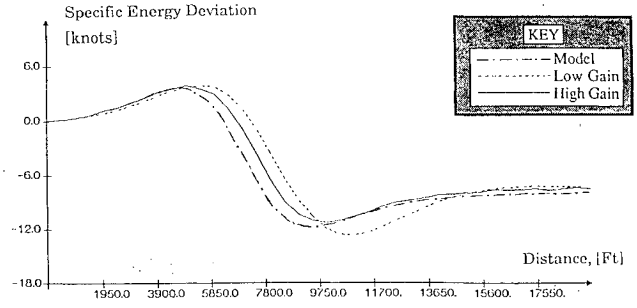

Fig. 6 Comparison of aircraft energy deviation due to headwind-tailwind shear and predicted energy deviation.

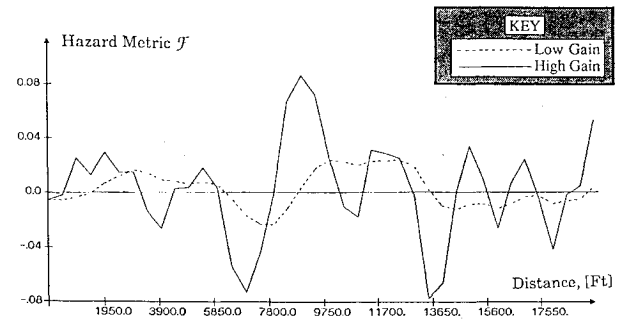

Fig. 7 Comparison of F-factor predictions in severe Dryden turbulence.

situation 10 s later, comparing the predicted hazard metric $\mathcal{F}_{av}$ along the flight path with the model's $\mathcal{F}_{av}$ component due to the headwind/tailwind shear alone. The predictions agree well with the model's head/tail wind component of $\mathcal{F}_{av}$, but the peak magnitude of the prediction is attenuated due to the finite bandwidth of the prediction algorithm. In addition, the distance between the aircraft and the wind shear is overpredicted due to phase shifting. With a lower value of σ_η, the estimators have lower gains, and these effects are more pronounced. If a wind shear warning were issued each time a critical value of $\mathcal{F}_{av}$ was exceeded, the algorithm with higher σ_η would have a greater chance of positively identifying severe wind shear.

For the same simulation, Fig. 6 compares the predicted energy deviation, normalized as an airspeed deviation, and the energy deviation due to the component of the wind shear. Although the error in prediction of distance to the microburst is greater for the lower value of σ_η, both predictions perform favorably in predicting peak energy loss. However, the total energy loss to the aircraft is greater than either prediction, due to the effect of the unobserved downdraft winds.

Figure 7 compares the predicted hazard metric $\mathcal{F}_{av}$ for each of the prediction designs in severe Dryden turbulence. The higher choice of σ_η results in greater response to turbulence. If wind shear warnings were issued each time a critical value of $\mathcal{F}_{av}$ was predicted, the algorithm with higher σ_η would issue more frequent false alarms. The optimization of a prediction algorithm must take into account both detection performance and false alarm prevention. Wavelengths corresponding to severe wind shear should be passed, but short wavelength disturbances that do not affect the flight path should be eliminated.

Conclusions

Doppler wind sensors can provide advance warning of a wind shear threat, but wind measurements are influenced by turbulence and measurement error. Optimal estimation provides a framework for minimizing the error of wind estimates given a hypothesis of the wind field structure. The estimation procedures presented here assume a structure to the local wind field at each range gate of the Doppler sensor, resulting in a bank of parallel Kalman filters. A first-order Markov turbulence model accounts for spatial correlation in the wind field due to turbulence. Measures of uncertainty are produced during the optimal estimation process. Stochastic prediction techniques are used to predict the impact of estimated winds on the energy performance of the aircraft. These techniques extend naturally to multiple Doppler sensors and could be expanded to predict other quantities such as altitude deviation error and touchdown dispersion error, given a nominal model of pilot compensation.

If wind shear warning is based on a critical threshold value of a hazard prediction, the detection reliability depends on the design of the prediction algorithm. Kalman-filter-based designs may be band limited, identifying areas with a sustained level of substantial wind shear. To further refine the algorithm, a comparative analysis of prediction algorithm designs can be conducted, using an ensemble of representative severe wind shear models. The potential for false warning in severe turbulence also can be compared. Both threshold and design bandwidth may be chosen to further optimize detection reliability.

Hazard prediction from Doppler sensors can provide the sole basis for a wind shear alert, but the lack of vertical wind estimates limits the alert's reliability. Other sources of information could improve the reliability of Doppler-based stochastic predictions through adaptive prediction techniques. Moreover, threshold exceedance of a hazard prediction could be viewed as uncertain evidence supporting a hypothesis of severe wind shear in the Bayesian network. With the reliability of threshold exceedance as evidence established through statistical analysis, hazard prediction can be incorporated into a probability-based expert system for wind shear avoidance.

Acknowledgment

This research has been sponsored by the NASA Langley Research Center under Grant NAG-1-834.

References

[1]Townsend, J., (ed.), *Low-Altitude Wind Shear and Its Hazard to Aviation,* National Academy Press, Washington, DC, 1983.

[2]*Windshear Training Aid,* U.S. Department of Transportation, Federal Aviation Administration, Associate Administrator for Development and Logistics, Washington, DC, Feb. 1987.

[3]Fujita, T. T., "The Downburst: Microburst and Macroburst," Satellite and Mesometeorology Research Project, University of Chicago, Chicago, IL, 1985.

[4]McCarthy, J., Roberts, R., and Schreiber, W., "JAWS Data Collection, Analysis Highlights, and Microburst Statistics," *Preprints, 21st Conference on Radar Meteorology,* American Meteorological Society, Boston, MA, 1983, pp. 596–601.

[5]Rinehart, R. E., and Isaminger, M. A., "Radar Characteristics of Microbursts in the Mid-South," *Preprints, 23rd Joint Conference on Radar Meteorology,* American Meteorological Society, Boston, MA, 1986, pp. J116–J119.

[6]Turnbull, D., McCarthy, J., Evans, J., and Zrnić, D., "The FAA Terminal Doppler Weather Radar (TDWR) Program," *Preprints, 3rd International Conference on the Aviation Weather System,* American Meteorological Society, Boston, MA, 1989, pp. 414–419.

[7]Barab, J. D., Page, R. D., Rosenburg, B. L., Zurinskas, T. E., and Smythe, G. R., "Evaluation of Enhancements to the Low Level Windshear Alert System (LLWAS) at Stapleton International Airport," Final Rept., DOT/FAA/PS-88/14, July 1987–March 1988.

[8]Campbell, S. D., and Olson, S., "Recognizing Low-Altitude Wind Shear Hazards from Doppler Weather Radar: An Artificial Intelligence Approach," *Journal of Atmospheric and Oceanic Technology,* Vol. 4, No. 1, March 1987, pp. 5–18.

[9]Campbell, S. D., "Microburst Precursor Recognition Using an Expert System Approach," *Preprints, Fourth International Conference on Interactive Information and Processing Systems for Meteorology, Oceanography, and Hydrology,* American Meteorological Society, Boston, MA, 1988.

[10]Roberts, R. D., and Wilson, J. D., "A Proposed Microburst Nowcasting Procedure Using Single-Doppler Radar," *Journal of Applied Meteorology,* Vol. 28, No. 4, April 1989, pp. 285–303.

[11]Saint, S., "The Missing Element in Wind Shear Protection," *Business Aircraft Meeting and Exposition,* Society of Automotive Engineers Rept. SAE 830715, April 1983.

[12]Zweifel, T., "Sensor Consideration in the Design of a Windshear Detection and Guidance System," *Aerospace Technology Conference and Exposition,* Society of Automotive Engineers Rept. SAE 881417, Oct. 1988.

[13]Bracalente, E. M., and Jones, W. R., "Airborne Doppler Radar Detection of Low Altitude Windshear," *Journal of Aircraft,* Vol. 27, No. 2, 1990, pp. 151–157.

[14]Targ, R., and Bowles, R. L., "Airborne LIDAR for Avoidance of Windshear Hazards," *Proceedings of the Second Combined Manufacturer's and Technology Airborne Windshear Review Meeting* (Williamsburg, VA), Vol. 1, Oct. 1988, pp. 369–377.

[15]Scott, W. B., "Researchers Develop Airborne Flir with Ability to Pinpoint Microbursts," *Aviation Week and Space Technology,* Feb. 17, 1990, pp. 69–71.

[16]Stengel, R. F., and Stratton, D. A., "An Expert System for Wind

Shear Avoidance," *Engineering Applications of Artificial Intelligence,* Vol. 2, No. 3, Sept. 1989, pp. 190–197.

[17]Stratton, D. A., and Stengel, R. F., "Probabilistic Reasoning for Intelligent Wind Shear Avoidance," *Proceedings of the 1990 AIAA Guidance, Navigation, and Control Conference,* AIAA, Washington, DC, 1990, pp. 1099–1107.

[18]Stengel, R. F., *Stochastic Optimal Control,* Wiley, New York, 1986.

[19]Anderson, B. D. O., and Moore, J. B., *Optimal Filtering,* Prentice-Hall, Englewood Cliffs, NJ, 1979.

[20]Bayes, T., "An Essay Towards Solving a Problem in the Doctrine of Chances," *Two Papers by Bayes,* Hafner, New York, 1963.

[21]Papoulis, A., *Probability, Random Variables, and Stochastic Processes,* McGraw-Hill, New York, 1984.

[22]Pearl, J., *Probabilistic Reasoning in Intelligent Systems: Networks of Plausible Inference,* Morgan Kaufmann, San Mateo, CA, 1988.

[23]Byrd, G. P., Proctor, F. H., and Bowles, R. L., "Evaluation of a Technique to Quantify Microburst Windshear Hazard Potential to Aircraft," *Proceedings of the 29th Conference on Decision and Control* (Honolulu, HI), Vol. 2, 1990, pp. 689–694.

[24]Proctor, F., "Model Comparison of July 7, 1990 Microburst," *Proceedings of the Third Combined Manufacturer's and Technology Airborne Windshear Review Meeting* (Williamsburg, VA), Vol. 1, 1990, pp. 81–103.

[25]Oseguera, R., and Bowles, R. L., "A Simple Analytic, 3-Dimensional Downburst Model Based on Boundary Layer Stagnation Flow," NASA TM-100632, July 1988.

[26]"Flying Qualities of Piloted Airplanes," Military Specification 8785-C, Wright-Patterson Air Force Base, OH, Nov. 1980.

[27]Hinton, D., "Flight Management Strategies for Escape from Microburst Encounters," NASA TM-4057, Aug. 1988.